Available online at www.sciencedirect.com
ScienceDirect
Acta Materialia 57 (2009) 1367–1372
Acta MATERIALIA
www.elsevier.com/locate/actamat

An instability index of shear band for plasticity in metallic glasses

Z. Han [a], W.F. Wu [a], Y. Li [a,*], Y.J. Wei [b], H.J. Gao [b,*]

[a] Department of Materials Science and Engineering, Faculty of Engineering, National University of Singapore, Engineering Drive 1, Singapore 117576, Singapore
[b] Division of Engineering, Brown University, 610 Barus & Holley, 182 Hope Street, Providence, RI 02912, USA

Received 8 October 2008; received in revised form 11 November 2008; accepted 13 November 2008
Available online 26 December 2008

Abstract

Catastrophic failure along a dominant shear band sets the limit on how much plasticity can be achieved in metallic glasses (MGs) under uniaxial compression. Here we show that this instability process is governed by a single system parameter, called the shear-band instability index (SBI), which is proportional to sample size and inversely proportional to machine stiffness. We provide extensive experimental proof of this concept by conducting a series of tests with a range of controlled values of sample size and machine stiffness. The theory of SBI has led us to a more comprehensive understanding of the mechanisms of plastic deformation in MGs via simultaneous operation of multiple shear bands versus a single dominant one. This concept provides a theoretical basis to design systems which promote plasticity/ductility in MGs by suppressing or delaying shear-band instability.

Keywords: Metallic glasses; Shear-band instability index; Plasticity; Size effect; Machine stiffness

1. Introduction

Metallic glasses (MGs), including highly processable bulk metallic glasses (BMGs), are a new class of engineering materials which have attracted significant technological interests [1–5]. Although many MGs exhibit high strength [6] and show substantial fracture toughness [7,8], their deformation mechanisms are fundamentally different from those of crystalline solids due to their lack of long-range atomic order in the former. Traditionally it is believed that under room temperature and uniaxial stress states, MGs deform through a process of highly localized shearing in narrow bands [9] and fail along one dominant shear band catastrophically in a geometrically unconstrained specimen [10]. A typical stress–strain curve of MGs exhibits only limited plastic strain of less than 2% [10]. Understanding the deformation and failure mechanisms [11–17] of shear bands, with the aim to improve the plasticity/ductility [16,18–21] of MGs, are of central interests for these materials.

There have been many attempts to describe the mechanism of plastic deformation in BMGs. Two of the earlier ones are the classical "free volume" model by Turnbull and co-workers [11,12] and Spaepen [13] and the "shear transformation zone" (STZ) model by Argon and Kuo [14]. Johnson and Samwer [15] proposed a cooperative shear model which placed more importance on the influence of shear modulus on the plastic flow of MGs. Recent studies have also shown a correlation between the plasticity and Poisson's ratio in these materials [16,17]. All of these viewpoints focused on the effects of intrinsic properties (i.e., atomic-level features in the structure) of MGs on their macroscopic deformation responses.

Here we note that the deformation and failure of MGs is really an instability process that begins with the nucleation and coalescence of STZs and ends up with the development and propagation of shear bands. Therefore, the instability process of shear-band failure ought to be a primary focus of study in understanding the deformation mechanism of MGs. For a material whose

* Corresponding authors.
E-mail addresses: mseliy@nus.edu.sg (Y. Li), Huajian_Gao@brown.edu (H.J. Gao).

1359-6454/$34.00 © 2008 Acta Materialia Inc. Published by Elsevier Ltd. All rights reserved.
doi:10.1016/j.actamat.2008.11.018

deformation hinges upon an instability process, inclusion of the influence of the testing machine besides that of the sample in the study of the apparent mechanical behaviors of the material is inevitable and unavoidable. The effect of machine stiffness has been previously mentioned by Murata et al. [22] and recently again by Xie and George [23], although a systematic and quantitative understanding on this issue is not yet available. Here we will first derive an instability index for shear-band failure in MGs from free energy changes in the sample–machine system. Through a series of carefully controlled experiments, we will show that the plasticity of monolithic BMGs depends strongly on the sample size as well as on the stiffness of the testing machine. An instability/stability map is established to show a critical transition from instability to stability as a function of sample size and machine stiffness. The stability is herein illustrated as the simultaneous operation of multiple shear bands, while the instability as the activation of a single dominant shear band. The significance of the instability index is to provide a definitive condition where the plasticity or even the ductility of BMGs can be obtained.

2. Experimental

Master alloy ingots with the nominal composition of $Zr_{64.13}Cu_{15.75}Ni_{10.12}Al_{10}$ [20] were prepared by arc-melting a mixture of high-purity metals in a Ti-gettered high-purity argon atmosphere. The ingots were then cast into rods with diameters from 1 to 4 mm by water-cooled copper mould low pressure casting. The amorphousity of these rods was checked by X-ray diffraction (XRD) and differential scanning calorimetry (DSC) (not shown here). The test samples were prepared to have a nominal aspect ratio of ~2:1. A few samples with an aspect ratio of ~1:1 were also prepared and tested. A custom designed device was used to grind the two ends of a sample to ensure that they are nearly parallel to each other within an accuracy of better than 10 μm and are perpendicular to the longitudinal axis of the sample. Uniaxial compression tests were conducted at room temperature with a constant strain rate of $4 \times 10^{-3}\,s^{-1}$ and a wide range of values for the machine stiffness between 22,800 and 159,000 N mm^{-1}. The machine stiffness was evaluated by running the compression test in the absence of a sample, and is taken to be the slope of the load–displacement curve. Since the stiffness is a function of load, we take the stiffness value corresponding to the load at the yield point for each sized sample.

3. The shear-band instability index (SBI)

To understand the shear-band instability, we consider a closed system consisting of a MG sample and an elastic spring representing the summary influence of the system outside the sample, primarily the testing machine (Fig. 1). When a displacement u is imposed on the sample–machine system, the change in elastic energy of the system is

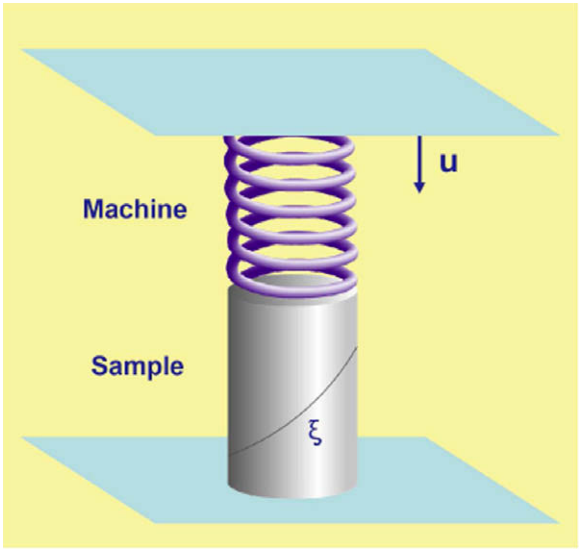

Fig. 1. Schematic representation of the sample–machine system, with u denoting a displacement imposed on the system, and ξ being an internal variable (e.g. the length or density of shear band) measuring the shear banding progress.

$$U = \frac{1}{2}\frac{u^2}{c_M + c_s} \tag{1}$$

where c_M and c_S are the compliances of the equipment and sample, respectively. Let ξ be an internal variable (e.g., the length or density of shear band) measuring the "progress" of shear banding. The rate of energy release during shear band formation is

$$G = -\frac{\partial U}{\partial \xi} = \frac{u^2}{2(c_S + c_M)^2} c_S' = \frac{1}{2}F^2 c_S' \tag{2}$$

where $F = u/(c_S + c_M)$ denotes the load on the sample, and $c_S' = \frac{\partial c_S}{\partial \xi} > 0$ since the compliance of the sample should increase with ξ in an instability process. The critical condition for shear band to progress can be expressed in terms of an energy criterion [24] as

$$G - G_c = 0 \tag{3}$$

where G_c denotes the intrinsic resistance of the material to shear banding. Furthermore, the condition for the shear band process to run unstably is

$$\frac{\partial (G - G_c)}{\partial \xi}\Big|_u > 0$$

Using $\frac{1}{2}F^2 c_S' = G_c$, it can be shown that

$$\left.\frac{\partial (G - G_c)}{\partial \xi}\right|_u = \frac{G_c c_S'}{c_S}\left(\frac{c_S'' c_S}{c_S'^2} - \frac{2}{1 + \frac{c_M}{c_S}}\right) = \frac{G_c c_S'}{c_S}\left(\frac{c_S'' c_S}{c_S'^2} - \frac{2}{1+S}\right) \tag{4}$$

where

$$S = c_M / c_S$$

is defined as the shear-band instability index (SBI). Eq. (4) suggests that the instability of a shear band is completely controlled by SBI as well as the property of the sample. The first term within the bracket on the right-hand side of Eq. (4) depends only on the material and geometrical properties of the sample and must be positive for an instability to develop; the second term within the bracket shows that SBI plays the role of a single controlling parameter for the onset of shear-band instability. For $c_S'' > 0$, $c_S' > 0$, there exists a critical SBI:

$$S_{cr} = \left(\frac{2c_S'^2}{c_S'' c_S}\right) - 1 \tag{5}$$

so that the instability condition $\frac{\partial(G-G_c)}{\partial \xi}|_u > 0$ is equivalent to

$$S > S_{cr} \tag{6}$$

In principle, it may be possible to determine S_{cr} from a first principles calculation based on a thorough understanding of the detailed physical mechanisms behind the shear-band instability. At the moment, this understanding is not yet available. On the other hand, we can treat S_{cr} as a phenomenological parameter to be determined from experiments and consider

$$S = \frac{c_M}{c_S} = \frac{\kappa_S}{\kappa_M} = \frac{\pi E_Y d}{4\rho\kappa_M} \tag{7}$$

as a single controlling parameter, where $\kappa_M (= c_M^{-1})$ is the stiffness of the testing machine, while $\kappa_S (= c_S^{-1})$, E_Y, d and ρ are the stiffness, Young's modulus, diameter and aspect ratio (height to diameter ratio) of the sample, respectively. When $S < S_{cr}$, the shear banding and the resulting deformation are expected to progress in a stable fashion. When $S > S_{cr}$, shear banding is unstable and the resulting deformation is expected to run unstably on one dominant shear band.

4. Experimental results

The concept of SBI suggests that the critical size for stable shear banding scales with the stiffness of the testing machine. It also indicates that for samples of the same size, higher machine stiffness will retard instability and thus results in more plasticity; for a given stiffness, smaller samples will show higher stability/plasticity. In order to verify the validity of these predictions, a series of tests were conducted with a range of controlled values of sample size and machine stiffness.

The measured stress–strain behaviors of 2:1 samples are plotted in Fig. 2 for different values of the machine stiffness and sample size (diameter). We identify that samples giving the stress–strain curves (marked with full circle) with a characteristic positive slope after yielding also show formation of multiple shear bands during deformation (see Fig. 3a). This means that no single shear band has run unstably in these samples, at least at the very initial stage of yielding. Therefore, we regard a positive slope of the

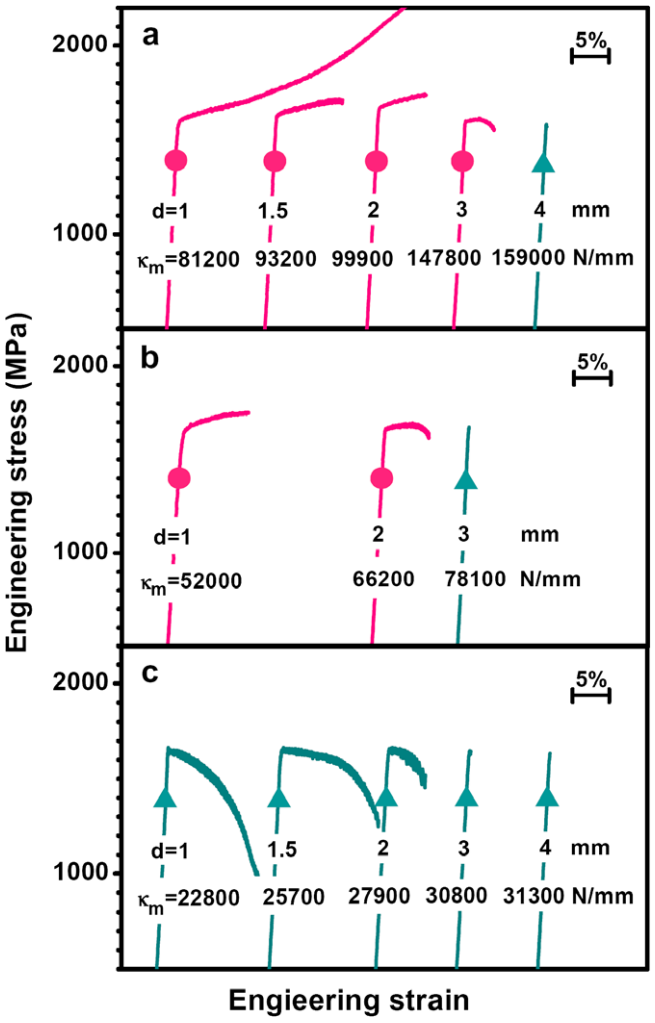

Fig. 2. Engineering stress–strain curves of 2:1 samples measured for a range of controlled values of sample size and machine stiffness. The curves with full circles represent stable behaviors, while curves with triangles represent unstable behaviors of shear banding. The sample diameter (d) and testing machine stiffness (κ_M) are both indicated in each curve.

stress–strain curve after yielding as a stable behavior. On the other hand, we find that samples with stress–strain curves (marked with triangle) either fail catastrophically with zero plasticity or slide progressively along a single dominant shear band (see Fig. 3b), resulting in a negative slope of the stress–strain curve on and after yielding. The formation of a single dominant shear band is taken as the evidence for unstable (run-way) behavior of shear banding. Generally, for a given machine stiffness, there is a transition from unstable to stable behavior when the sample size is reduced. As seen in Fig. 2a and b, the maximum plastic strain before failure increases as the sample size is reduced from 4 to 1 mm, and the stress–strain curve shows positive slope at yielding. More significantly, the stiffness of the testing machine also shows a strong influence on the test results. When the stiffness of the machine was increased, the same sized sample started to exhibit better stability (more plasticity). For example, the 1 mm sample tested at a machine stiffness of 22,800 N mm^{-1} showed

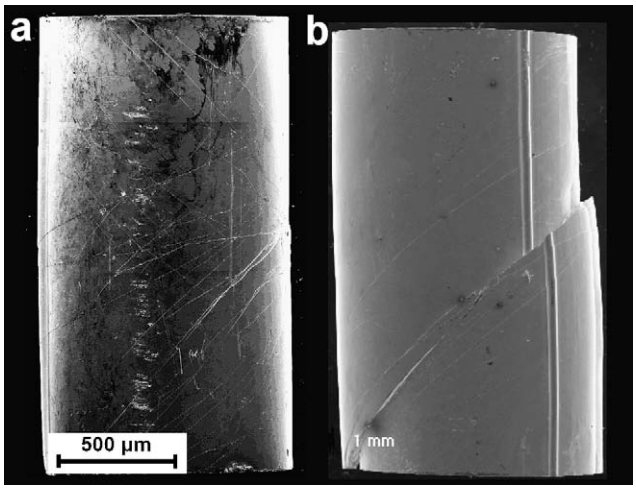

Fig. 3. SEM micrographs of 1 mm 2:1 samples tested at a machine stiffness of (a) 81,200 N mm^{-1}, exhibiting a stable behavior of shear banding by forming multiple shear bands in multiple maximum shearing directions throughout the sample, and (b) 22,800 N mm^{-1}, exhibiting an unstable behavior of shear banding by forming one dominant shear band, respectively.

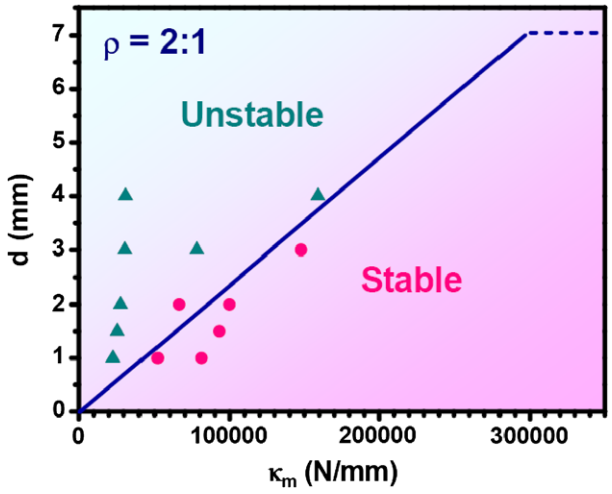

Fig. 4. A stability/instability map with respect to the sample size (d) and machine stiffness (κ_M) for 2:1 samples.

an unstable behavior by failing along one dominant shear band as shown in Fig. 3b, while the same sized sample tested at a stiffness of 52,000 N mm^{-1} showed a stable behavior at least before a plastic strain of 5%. The extreme case of this study is that when the machine stiffness is further increased to 81,200 N mm^{-1}, the same sample can be compressed to beyond 25% plastic strain with uniformly distributed shear bands without failure. This test was repeated 10 times, and 9 out of 10 samples exhibited such behavior. In this situation, the sample deforms continuously by simultaneous operation of multiple shear bands (Fig. 3a).

The above stable/unstable behaviors are summarized in Fig. 4. There are clearly distinct stable and unstable regions reasonably separated by a straight line, in agreement with

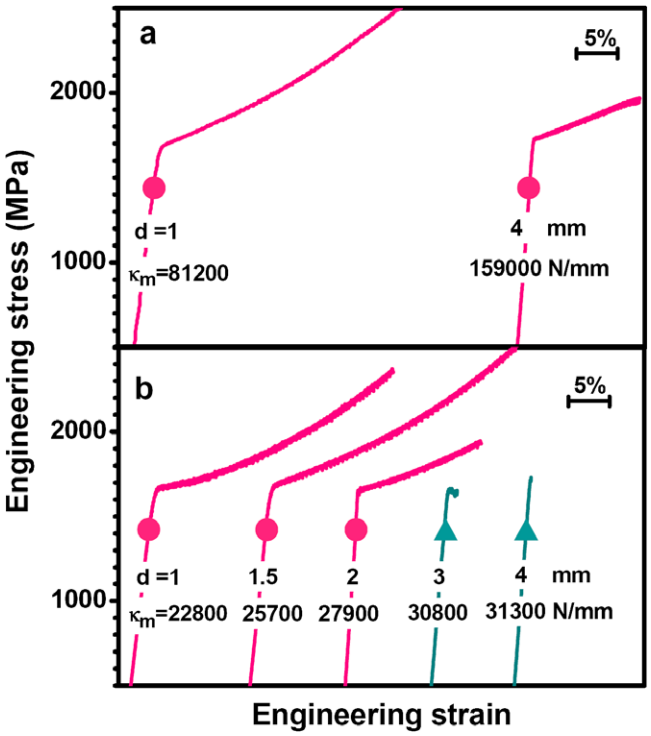

Fig. 5. Engineering stress–strain curves of 1:1 samples measured for a range of controlled values of sample size and machine stiffness.

the predictions based on SBI. The slope of the dividing line shows that the value of critical S for the MGs under study is around 0.72 (using $E_Y = 78$ GPa in Eq. (6)) for the samples with an aspect ratio of 2. The significance of the dashed line will be discussed in Section 5.2.

To further verify this concept, a series of samples with a diameter of 1 to 4 mm and an aspect ratio of 1 were compressed for different values of the machine stiffness, similar to those shown in Fig. 2. The measured stress–strain behaviors are plotted in Fig. 5. It was found that the 3 mm sample tested at a stiffness of 30,800 N mm^{-1} and the 4 mm sample tested at a stiffness of 31,300 N mm^{-1} still failed through the unstable mode (see Fig. 6a), while the rest of

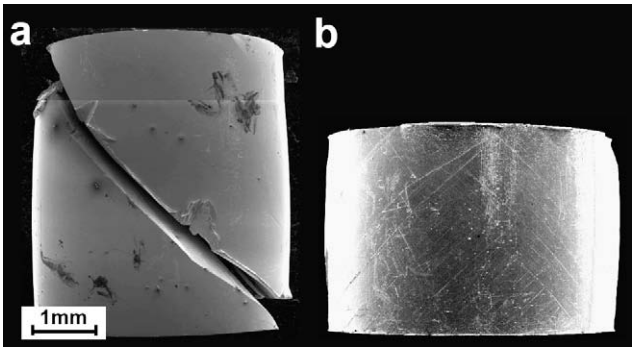

Fig. 6. SEM micrographs of 4 mm 1:1 samples tested at a machine stiffness of (a) 31,300 N mm^{-1}, exhibiting an unstable behavior of shear banding by forming one dominant shear band, and (b) 159,000 N mm^{-1}, exhibiting a stable behavior of shear banding by forming dense shear bands, and thus uniform deformation, respectively.

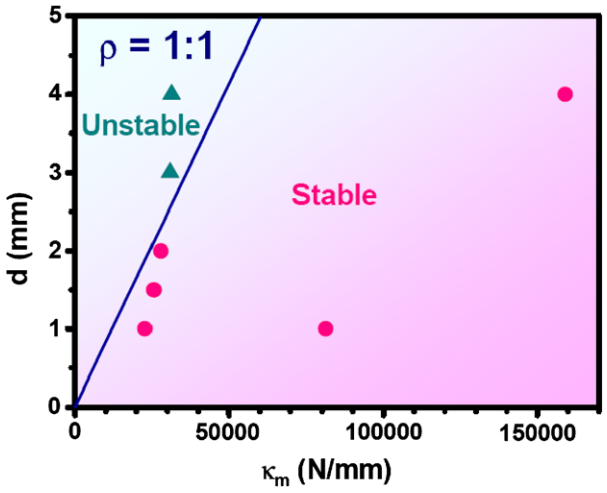

Fig. 7. A stability/instability map with respect to the sample size (d) and machine stiffness (κ_M) for 1:1 samples.

samples tested all exhibited stable behavior (see Fig. 6b). The stable/unstable behaviors for 1:1 samples are summarized in Fig. 7. With a steeper division line separating the instability/stability regions, the critical S calculated for 1:1 samples is ~4.

5. Discussion

5.1. The effect of machine stiffness

Figs. 4 and 7 can serve as stability/instability maps with respect to the sample size and machine stiffness, showing where conditions in favor of stable plastic deformation can be obtained. For a fixed sample aspect ratio ρ and Young's modulus E_Y, higher machine stiffness κ_M and smaller sample size d tend to decrease S and suppress the formation of one dominant shear band, thereby promoting simultaneous operation of multiple shear bands. Oppositely, lower machine stiffness and larger sample size tend to increase S and promote the formation of a single dominant shear band. The extreme case of zero machine stiffness $\kappa_M = 0$, in which case a very large amount of elastic energy is stored in the test machine (i.e., $E_M = \infty$), corresponds to a load-controlled testing condition which tends to promote instability whenever a softening mechanism exists. The opposite case of infinite machine stiffness $\kappa_M = \infty$, in which case $E_M = 0$, corresponds to the displacement-controlled testing condition which tends to suppress brittle instability.

Most previous studies on the plastic deformation of monolithic BMGs may have ignored the influence of the testing machine. It is noted that even for our best case with the lowest S, i.e. the 1 mm sample tested at a machine stiffness of 81,200 N mm^{-1}, the energy stored in the machine is still a sizable 38% of that in the sample. For the 4 mm sample tested at a stiffness of 31,300 N mm^{-1}, the energy stored in the machine is nearly 4 times that of the sample. This indicates that perhaps most of the reported results in the literature are under strong influence of the testing machine, just to different degrees. Furthermore, the concept of SBI indicates that even small monolithic MG samples, perhaps right down to the micrometer range, can still fail either stably or unstably depending on the machine stiffness. This seems consistent with a few reports [25–27]. Of course when the sample becomes extremely small (e.g. on the order of shear-band width), other factors may intervene. Another point worth noting here is that MGs with different intrinsic malleability may possess distinct values of the critical SBI which can only be obtained from experiments. The widely observed brittle BMG systems, such as Fe- [28,29], and Mg-based [30] systems are supposed to have very low critical SBI, while several Pt- [16], Zr- [20], and Cu-based [31] alloys, which have been reported to be plastic, are predicted to exhibit high critical SBI.

5.2. The upper size limit for stability and intrinsic size effect

We point out that the theory of SBI has so far only been established for a quasi-static system. For large samples, dynamic energy transport is of growing importance and it may be necessary to extend this concept to a fully dynamic system. For example, even in the case of infinite machine stiffness, it is conceivable that the sample may still exhibit an intrinsic size effect in the sense that, when the sample size is larger than a critical one, the energy stored in the sample itself will be sufficient to promote a single dominant shear-band. It should be possible to work out an upper limit size d_c under $\kappa_M = \infty$, if the critical fracture energy γ_c, which equals to the total energy E_T released upon failure divided by the total fracture area A in brittle fracture, is estimated. It is found in Fig. 2a for 2:1 samples that the 4 mm sample begins to fail without any apparent plasticity. Assuming 4 mm is the critical size for brittle fracture under a given machine stiffness, the critical fracture energy is consequently estimated as

$$\gamma_c = \frac{E_T}{A} = \frac{E_M + E_S}{A} = \frac{0.77E_S + E_S}{A} = \frac{1.77 \times d \times \frac{\sigma^2}{E_Y}}{2\sqrt{2}} \qquad (8)$$

where the elastic energy stored in the sample is

$$E_S = \frac{1}{2}\int_V \sigma_{ij}\varepsilon_{ij}\,dV = \frac{\pi d^3}{4}\cdot\frac{\sigma^2}{E_Y}$$

and the elastic energy stored in the machine is $E_M = E_S\kappa_S/\kappa_M = 0.77E_S$, $A = \sqrt{2}\pi d^2/2$ by taking the shear plane to be 45° with respect to the loading axis, $d = 4$ mm, and σ is the yield strength in uniaxial compression. With the critical fracture energy estimated from Eq. (8), when $\kappa_M = \infty$, and thus $E_T = E_S$, the upper limit size is calculated to be $d_c = 1.77\ d = 7.08$ mm. Therefore, for the present $Zr_{64.13}Cu_{15.75}Ni_{10.12}Al_{10}$ BMG with an aspect ratio of 2 under $\kappa_M = \infty$, the critical diameter beyond which the stable shear banding cannot be achieved whatsoever, is

predicted to be around 7 mm. This provides an upper limit for the stability region in the map shown in Fig. 4.

5.3. The effect of the sample aspect ratio

The critical S determined for 1:1 samples is more than 5 times larger than that for 2:1 samples. It is apparent that the larger the critical S, the easier the stable behavior can be achieved. This explains why 1:1 samples have been widely observed to be stable. Our findings point out that stable shear banding cannot be obtained in sufficiently large samples and simultaneously at low machine stiffness even for samples with an aspect ratio of 1:1. The unstable mode exhibited by the 3 and 4 mm 1:1 sample suggests that the machine stiffness, i.e. the energy stored in the testing machine, has a stronger influence on the mechanical behavior of MG samples than the geometrical confinement.

6. Conclusion

Our present study has shown, both theoretically and experimentally, that the failure of MGs by shear band formation is governed by a single instability index which depends on both the stiffness of the testing machine and the size of the sample. This index sets the condition where plasticity in BMGs can be obtained, i.e. small samples on stiff machines. Since most of the previously reported results on the mechanical behavior of MGs are perhaps entirely interpreted without incorporating the influence of the testing machine, the concept of SBI is of fundamental importance for a shift of paradigm in the future study of MGs. We also note that the deformation mechanisms reported here should not be limited to compressive responses of monolithic BMGs. Sustained tensile ductility may also be achievable under sufficiently small sample size and large enough machine stiffness. This is currently under investigation.

References

[1] Peker A, Johnson WL. Appl Phys Lett 1993;63:2342.
[2] Inoue A. Acta Mater 2000;48:279.
[3] Li Y, Poon SJ, Shiflet GJ, Xu J, Kim DH, Loffler JF. MRS Bull 2007;32:624.
[4] Greer AL. Science 1995;267:1947.
[5] Wu WF, Li Y, Schuh CA. Philos Mag 2008;88:71.
[6] Inoue A, Shen BL, Koshiba H, Kato H, Yavari AR. Nat Mater 2003;2:661.
[7] Gilbert CJ, Ritchie RO, Johnson WL. Appl Phys Lett 1997;71:476.
[8] Yavari AR, Lewandowski JJ, Eckert J. MRS Bull 2007;32:635.
[9] Zhang Y, Greer AL. Appl Phys Lett 2006;89:071907.
[10] Leamy HJ, Chen HS, Wang TT. Metall Trans 1971;3:699.
[11] Cohen MH, Turnbull D. J Chem Phys 1959;31:1164.
[12] Polk DE, Turnbull D. Acta Metall 1972;20:493.
[13] Spaepen F. Acta Metall 1977;25:407.
[14] Argon AS, Kuo HY. Mater Sci Eng 1979;39:101.
[15] Johnson WL, Samwer K. Phys Rev Lett 2005;95:195501.
[16] Schroers J, Johnson WL. Phys Rev Lett 2004;93:255506.
[17] Lewandowski JJ, Wang WH, Greer AL. Phil Mag Lett 2005;85:77.
[18] Schuh CA, Hufnagel TC, Ramamurty U. Acta Mater 2007;55:4067.
[19] Das J, Tang MB, Kim KB, Theissmann R, Baier F, Wang WH, Eckert J. J Phys Rev Lett 2005;94:205501.
[20] Liu YH, Wang G, Wang RJ, Zhao DQ, Pan MX, Wang WH. Science 2007;315:1385.
[21] Hofmann DC, Suh JY, Wiest A, Duan G, Lind ML, Demetriou MD, Johnson WL. Nature 2008;451:1085.
[22] Murata T, Masumoto T, Sakai M. In: Cantor B, editor. Rapidly quenched metals III, vol. 2; 1978. p. 401.
[23] Xie S, George EP. Intermetallics 2008;16:485.
[24] Hellan K. Introduction to fracture mechanics. NY: McGraw-Hill; 1984 [chapter 4].
[25] Volkert CA, Donohue A, Spaepen F. J Appl Phys 2008;103:083539.
[26] Schuster BE, Wei Q, Hufnagel TC, Ramesh KT. Acta Mater 2008;56:5091.
[27] Guo H, Yan PF, Wang YB, Tan J, Zhang ZF, Sui ML, et al. Nat Mater 2007;6:735.
[28] Gu XJ, McDermott AG, Poon SJ, Shiflet GJ. Appl Phys Lett 2006;88:211905.
[29] Yao JH, Wang JQ, Li Y. Appl Phys Lett 2008;92:251906.
[30] Xi XK, Zhao DQ, Pan MX, Wang WH, Wu Y, Lewandowski JJ. Phys Rev Lett 2005;94:125510.
[31] Jia P, Guo H, Li Y, Xu J, Ma E. Scripta Mater 2006;54:2165.